Waste Management 131 (2021) 423–432

Contents lists available at ScienceDirect

Waste Management

journal homepage: www.elsevier.com/locate/wasman

Upcycling polyamide containing post-consumer Tetra Pak carton packaging to valuable chemicals and recyclable polymer

Xiaolin Chen, Yixin Luo, Xianglan Bai *

Department of Mechanical Engineering, Iowa State University, Ames, IA, USA

ARTICLE INFO

Keywords:
Tetra Pak
Recycling
Levoglucosenone
Furfural
Caprolactam
Polyethylene

ABSTRACT

Billion tons of post-consumer Tetra Pak cartons are discarded annually as land and ocean wastes, creating significant environmental problems and resource losses. Recycling of the carton wastes is hindered by its multi-material compositions and low values of the recycled products. In this study, a novel upcycling of the cartons was investigated. A post-consumer carton consisting of paper, polyolefin, and polyamide was directly converted in 210–230 °C tetrahydrofuran containing 10–20 mM acid to produce up to 19.2% of levoglucosenone and 8.6% of furfural by selectively decomposing paper fraction. The remaining solids containing mostly intact polyethylene and polyamide but also a smaller fraction of paper-derived char were separated using a solvent-dissolution method. The xylene-soluble fraction was a recycled polymer similar to the original polyethylene, which was verified by its functional groups, the composition of the pyrolysis products, and the melt rheology results. The xylene-insoluble fraction was a mixture of polyamide and paper-derived char. Upon pyrolysis, caprolactam was produced as the only major vapor product. The remaining, thermally stable paper-derived char could be used as a high-quality solid fuel. Overall, the demonstrated recycling method could potentially maximize the values of the products recovered from carton wastes.

1. Introduction

Increasing human activities over the past several decades created enormous amounts of end-of-life materials requiring disposal. Most of them are currently sent to landfills or end up as land/ocean wastes, which cause numerous environmental problems and human health issues (Ayiania et al., 2019; Jambeck et al., 2015; Dimitris S. et al., 2012). While recycling is the most promising way to reduce the problems caused by improper disposal of wastes, the lack of efficient recycling technology greatly hinders the motivation for waste recycling (Polprasert, 2007). Compared to single material-made wastes, composite wastes are much more challenging to recycle either mechanically or chemically due to the inconsistency in the chemical composition and material properties (Yang et al., 2012). Tetra Pak cartons are such an example; ever since it was introduced in the market in 1952, Tetra Pak quickly became one of the most popular packaging materials for storing foods and beverages (Zawadiak, 2017). Tetra Pak cartons are multilayer laminated composites. While they are usually made of 75% paper, 20% low density polyethylene (PE), and 5% aluminum, aluminum can be absent in the cartons used in short-term storage products, such as refrigerated milk, juice, cream, egg substitutes, soy and grain milk (Zawadiak et al., 2017; Carton Facts). Polymers other than PE are also added to cartons to meet specific product requirements. For example, adding a polyamide (PA) layer in cartons can prevent flavor loss and eliminate odor (Kamal et al., 1984). Currently, more than 190 billion carton packages are used worldwide annually, among which only 26% of post-consumer cartons (PCC) are recycled by the carton manufacturer, and the rest are sent to landfill or burned (Tetra Pak International, 2020). The billion tons of discarded PCC are not only the source of environmental pollutions but also an abandoned resource. Thus, recycling PCC to reclaim its value is important in terms of environmental protection and resource recovery. PCC recycling is hindered due to its multi-material compositions and the economy of the process (Krauklis et al., 2021; Delvere et al., 2019; Henshaw et al., 1996). So far, both mechanical and chemical recycling methods of PCC were explored (Martinez-Barrera et al., 2019). For mechanical recycling, hydropulping of PCC in modified paper mills has been performed (Robertson, 2021). The paper fraction in PCC was removed by continuous agitation in water, leaving PE/Aluminum layers containing up to 5% residue paper fibre (Zawadiak et al., 2017). The recovered cellulosic fibers are usually

* Corresponding author.
E-mail address: bxl9801@iastate.edu (X. Bai).

https://doi.org/10.1016/j.wasman.2021.06.031
Received 6 April 2021; Received in revised form 28 June 2021; Accepted 29 June 2021

used for producing tissue, paper towel, fine writing paper, and other consumer products. Previously, the paper fraction in PCC was acid hydrolyzed to produce nanocrystalline cellulose (Xing et al., 2018). The recycled cellulose was also used in composite applications as a biobased filler (Platnieks et al., 2020). PE/aluminum product was combusted or pyrolyzed for heat and energy products during which aluminum could be recovered (European Commission; Korkmaz et al., 2009). The PE/aluminum layers were also hot-pressed for obtaining composite products (Lopes & Felisberti, 2006; Popelka et al., 2016). However, the recycled material was difficult to market due to the high energy consumption and/or poor product quality. To improve the quality of the recycled materials, solvent-based dissolution methods were applied to the hydropulped PCC to extract relatively pure PE and separate aluminum (Kaiser et al., 2017; Zhao et al., 2018; Achilias et al., 2007; Achilias et al., 2009). Nevertheless, recycling Tetra Pak cartons by this two-step mechanical method was reported to be costly and less likely profitable; although it is possible to recover high-quality precipitated polymer using solvent-based dissolution, all insoluble components remain as invaluable residues (Kaiser et al., 2017). Pyrolysis is a method to chemically recycle PCC. In a previous study, PCC was pyrolyzed under an inert environment with temperatures up to 600 °C to produce aqueous liquid and wax (Korkmaz et al., 2009). The wax mainly derived from the PE fraction contained paraffin, aromatics, and olefins. On the other hand, the aqueous phase containing phenols was derived from the paper fraction. Since the pyrolysis oil of PCC is an intermediate product with high oxygen content, catalytic pyrolysis was also performed using acid catalysts to deoxygenate vapors to produce aromatic hydrocarbon mixtures (Siddiqui et al., 2020). The applications of the pyrolysis char as an absorbent or soil amendment were also investigated (Raclavská et al., 2018). Instead of pyrolysis, PCC was also hydrothermally treated to produce hydrochar as a solid fuel (Baskoro Lokahita et al., 2017). Overall, most of the prior approaches either downcycled PCC to lower-value products using high energy inputs or partially utilizing PCC. Especially, recycling PCC for energy products is less attractive since the major fraction of PCC is paper, which has a low heating value.

Upcycling PCC for higher-value products can be a promising way to improve economic feasibility and promote recycling activities. Ideally, multiple products are developed from PCC based on the chemical compositions and/or the material properties of the PCC constituents for the maximized product values. While paper, which accounts for 75–80% of PCC, is made of cellulose, cellulose is an excellent feedstock for producing biobased chemicals (A et al., 2020; He et al., 2017; Cao et al., 2015). Thus, PCC can be a low-cost feedstock for high-valued chemicals if a proper recycling method is developed. In this study, we explored a novel integrated upcycling approach to produce both chemicals and polymers from PCC. The PCC used in this study does not contain aluminum, but it was made of paper, PE, and PA. The PCC was first pretreated with tetrahydrofuran (THF) to selectively convert its paper fraction into biobased chemicals, namely levoglucosenone (LGO) and furfural. The remaining solids consisting of PE, PA, and the paper-derived char were further processed by a solvent-dissolution method to recover a polymer whose properties are similar to the original PE. Additionally, the PE-recovered, remaining solid consisting of the paper-derived char and PA was pyrolyzed to recover caprolactam, a precursor monomer of nylon-66. The schematic diagram of the recycling approach in this study is illustrated in Fig. 1.

2. Materials and methods

2.1. Materials

PCC was collected from a refrigerated milk container (i.e., Horizon Organic Milk) purchased from a local grocery store. The manufacturer of the carton is Tetra Pak. Ultimate analysis and proximate analysis of PCC are given in Table S1. According to our lab analysis, it contained 80% of paper, 17% of PE, and 3% of PA. HPLC grade THF stabilized with 0.025% butylated hydroxytoluene (BHT) and sulfuric acid were purchased from Fisher Chemical. LGO was purchased from GlycoSyn. Levoglucosan (LGA) was purchased from Fisher-Scientific company, Inc. Furfural and 1,4:3,6-dianhydro-α-D-glucopyranose (DGP), xylene and

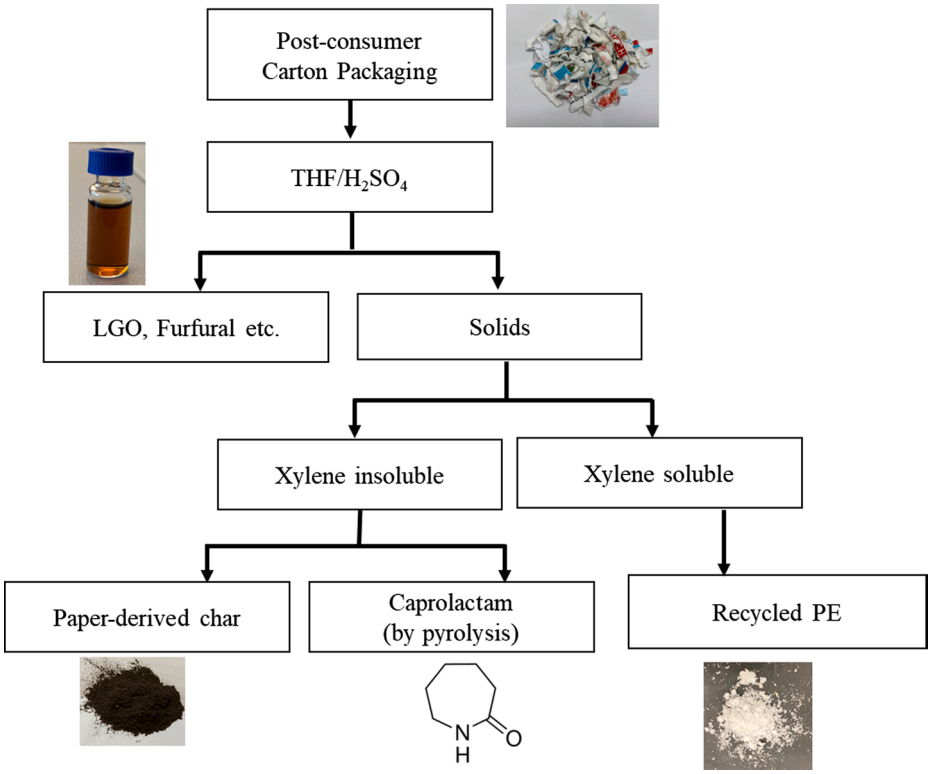

Fig. 1. Summary of PCC recycling approach.

propanol were purchased from Sigma-Aldrich.

2.2. Pretreatment of PCC in THF solvent

PCC was ball-milled into small pieces with a diameter of about 1 mm. The pretreatment of PCC in THF solvent was performed using 316 stainless-steel Swagelok reactors assembled using two 1/2 in. plugs and a 1/2 in. port connector. The inner volume of the reactor was 3 mL. For each experiment, 12 ~ 36 mg of PCC and 2 mL of THF were added to the reactors. Calculated amounts of sulfuric acid were added to obtain the solution with the desired acid concentrations. The sealed reactors were shaken for 5 mins prior to the conversion to make sure that PCC particles and the solvents were in good contact. An industrial fluidized sand bath was used to supply heat for the conversion. After the sand bath reached the preset reaction temperatures, the reactors were dropped into the sand bath for heating. When the desired reaction time was reached, the reactors were quickly taken out of the sand bath and immediately quenched in a water bath at room temperature. The reaction time was counted starting from when the reactors entered the sand bath until they were removed for the quenching.

The liquid and solid suspension inside the reactor were extracted using a glass syringe and filtrated using a 0.45 μm glass fiber filter. The filtrate was stored for further characterization, and the solid residue was dried at 40 °C inside a vacuum oven overnight before it was weighted. The gas yield was negligible in all the tested cases, determined by weighing unsealed reactors before and after the reactions. Thus, the product yields were determined using the equations given below:

$$\text{Solid yield } (\%) = \frac{\text{mass of solid residue}}{\text{total mass of feedstock}}$$

$$\text{Liquid yield } (\%) = 100\% - \text{solid yield } (\%)$$

2.3. Solvent-dissolution separation of THF-pretreated solids

The solids obtained from the THF pretreatment above were further separated using a non-polar and polar solvents combined method similar to it was described in previous studies (Georgiopoulou et al., 2021; Pappa et al., 2001). First, the pretreated solids and xylene were mixed at a ratio of 1:15 (g/mL) in a beaker. The mixture was heated to 85 °C for 2 hrs with a stirring rate of 300 rpm. The hot solution was filtrated to remove insoluble materials. Subsequently, a three-times volume of 1-propanol was added to the filtered solution dropwise to precipitate the xylene soluble products. The above process was repeated twice before both the soluble and insoluble products were dried overnight to remove residue solvents.

2.4. Hydropulping of PCC

In this study, the original PCC (untreated) was also subjected to hydropulping to remove the paper fraction and recover water-insoluble materials consisting of PE and PA (Georgiopoulou et al., 2021). PCC was cut into small pieces (1 cm × 1 cm) and then mixed with water at a ratio of 1:30 (g/L). The mixture was stirred at 500 rpm for 5 hrs at ambient temperature. The paper pulp and the synthetic polymers were separated by centrifuge. After most of the pulps were removed by the initial filtration, the solution and water-insoluble polymers were further stirred for an additional hour to further remove the residual pulp fiber. Finally, the water-insoluble materials containing PE and PA were dried overnight inside a vacuum oven.

2.5. GC–MS analysis

The chemical composition of the liquid products obtained during the THF treatment of PCC was analyzed using an Agilent 7890B Gas Chromatograph (GC) equipped with Mass Spectrometer (MS) and Flame Ionization Detector (FID) equipped with two ZB-1701 (60 m × 250 μm × 0.25 μm) capillary columns. Initially, the GC oven temperature was held at 40 °C for 3 mins and then increased to 280 °C at 4 °C/min. Finally, the oven was held at the final temperature for additional 4 mins. Helium was the carrier gas with the column flow rate of 1 mL/min and the split ratio of 20:1 at the GC inlet. The chemical composition of the liquid products was identified with MS and quantified by FID. The compounds were quantified based on calibration curves created using their authentic chemicals. For each chemical, a five-point calibration was performed to achieve a regression coefficient higher than 0.99.

2.6. Fast pyrolysis

Fast pyrolysis was performed using a micro-pyrolyzer system (Rx-3050 TR, Frontier Laboratory, Japan) connected to an Agilent GC/MS-FID system same as described above. About 250 μg of sample in a deactivated stainless cup was pyrolyzed at 500 °C using helium as the pyrolysis gas. The pyrolysis vapors were then swept into the GC/MS-FID for product analysis. The flow rate of helium at the front inlet of the GC was 156 mL/min, and the split ratio was 50:1. The GC heating profile was the same as described above.

2.7. FTIR analysis

FTIR analysis was conducted using a Thermo Scientific Nicolet iS10 (Thermo Fisher Scientific Inc., Waltham, MA) equipped with a Smart iTR accessory. The wavenumbers of the FTIR analysis ranged from 750 cm^{-1} to 4000 cm^{-1}. The sample was scanned 32 times at a resolution of 4 cm^{-1} and an interval of 1 cm^{-1}.

2.8. Elemental analysis

Elemental analysis was conducted using a CHNS elemental analyzer (Vario Micro Cube) to determine the composition of carbon, hydrogen, nitrogen, and oxygen on a moisture-free basis. Oxygen content was determined by the mass difference. The high heating value (HHV) was calculated using Dulong's formula.

2.9. Thermogravimetric analysis (TGA)

TGA analysis was performed using a Mettler Toledo Thermogravimetry/Differential Scanning Calorimetry system (TGA/DSC). About 20 mg of sample was placed inside an alumina pan and heated from room temperature to 105 °C at a heating rate of 10 °C/min. The sample stayed at 105 °C for 40 min to remove moisture and/or low-boiling volatiles. The sample was then continually heated from 105 °C to 900 °C at a heating rate of 10 °C/min. Nitrogen gas with a flow rate of 100 mL/min was used as the sweep gas.

2.10. Melt rheology

Isochronal dynamic temperature sweep was performed using a Discovery hybrid rheometer (DHR-2, TA Instruments) with 25 mm parallel plate geometry. Temperature ramps were conducted with a maximum temperature of 250 °C, fixed angular frequency of 10 rad/s, and strain of 1.25%.

3. Results and discussions

3.1. Selective decomposition of PCC by THF pretreatment

3.1.1. Effect of acid concentration

The PCC particles were converted in 210 °C THF solvents with acid concentrations ranging from 10 to 20 mM. The mass balance of the products is given in Fig. 2(a) as a function of reaction time. While more than 50% of PCC decomposed in the first 45 mins reaction for all the

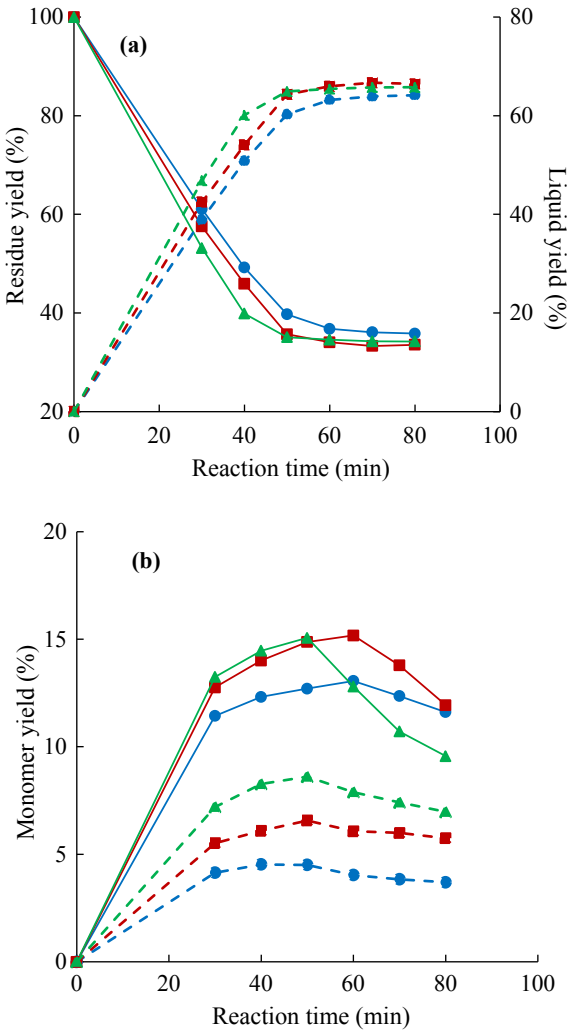

Fig. 2. Effect of acid concentration during THF pretreatment of PCC at 210 °C. Blue lines with ●: 10 mM acid; red line with ■: 15 mM acid; green lines with ▲: 20 mM acid. (a). liquid (dotted lines) and solid yields (solid lines); (b). LGO (solid lines) and furfural yields (dotted lines). (For interpretation of the references to colour in this figure legend, the reader is referred to the web version of this article.)

cases, its decomposition rate was positively correlated to acid concentration. After 45 mins, there were no significant changes in solid and liquid yields regardless of the acid concentrations. The liquid yields were similar for 15 mM and 20 mM acids, about 65% at 50 mins. In comparison, the liquid yield was slightly lower with the 10 mM acid.

In the liquid products, LGO was the major monomer in the liquid, followed by furfural. Their yields are shown in Fig. 2(b). LGO is a high-valued biobased molecule that has applications in pharmaceuticals, the synthesis of biobased solvents, and polymers (M. Sarotti et al., 2012; Corne et al., 2013; Ostermeier & Schobert, 2014; Müller et al., 2009). In previous studies, LGO was produced from cellulose or lignocellulosic biomass using catalytic pyrolysis or solvent-based conversion (Cao et al., 2015; Kudo et al., 2011; Kudo et al., 2016; Lu et al., 2014; Zhang et al., 2015). Furfural is also an important platform chemical widely used in solvents, polymers, and chemical synthesis (Cai et al., 2013; Machado et al., 2016). The maximum LGO yield of 15.2% (per the PCC mass) was obtained with the 15 mM acid solution after 60 mins. The LGO yields obtained with the 20 mM and 15 mM acid solutions were similar at the initial stage of the reactions. However, the higher acid concentration in the solution made LGO increasingly unstable at longer reaction times. On the other hand, furfural yield was promoted as the acid concentration in the solutions increased. A maximum furfural yield of 8.1% was obtained with the 20 mM acid solution. Other than LGO and furfural, DGP and levoglucosan (LGA) were also produced but with much lower yields. Their yields are given in Figure S1. THF is a polar aprotic solvent. Unlike polar protic solvents, aprotic solvents do not donate hydrogen. Since caging effect of hydrogen ions in protic solvents does not occur with aprotic solvents, acid-catalyzed reactions are strongly enhanced in aprotic solvents even in the presence of a very small amount of acid (Mellmer et al., 2014). Aprotic solvents were previously used to convert biomass to produce various products such as soluble sugars, LGO, LGA, hydroxymethyfuran, and furfural (Bai et al., 2014; Cao et al., 2015; Ghosh et al., 2016; Ghosh et al., 2018; He et al., 2017; Weingarten et al., 2014; Cai et al., 2014; Cai et al., 2013). It has shown that the conversion in aprotic solvents can also lower the activation energy required to depolymerize the glycosidic chain in cellulose compared to pyrolysis (Ghosh et al., 2016). Biomass conversion in aprotic solvents is unique also because the product selectivity can be tailored by choosing the solvent type and tuning acid concentration. Usually, a higher polarity of solvent enhances cellulose depolymerization to soluble sugars, whereas dehydration products are promoted with a lower solvent polarity (Ghosh et al., 2016). When the same type of solvent is used, low acid concentrations promote depolymerization reactions to produce LGA and soluble sugar oligomers, whereas increased acid concentrations preferentially produce LGO. On the other hand, furfural production is promoted by using water as a co-solvent of the aprotic solvents (Braden & Bai, 2018; Cai et al., 2013; Cai et al., 2014). Among various aprotic solvents, THF is particularly promising in converting cellulosic feedstock. It is a biomass-derivable green solvent with a moderately high polarity parameter. It also has a low boiling point of 66 °C, allowing the used solvent to be recovered using low energy. LGO and furfural were produced preferentially in this study, suggesting dehydrations are the dominant reactions. It has been suggested that the glycosidic chain of cellulose is first depolymerized to oligomer units and LGA which further dehydrated into LGO via DGP as a precursor (Cao et al., 2015; Hu et al., 2020). Furfural can be produced directly from the cellulose chain by dehydration or as a secondary reaction product of LGO and LGA. The reaction mechanisms of cellulose depolymerization and dehydration were described in previous publications (Cao et al., 2015; Ghosh et al., 2016; Ghosh et al., 2018).

3.1.2. *Effect of solvent temperature*

The effect of the solvent temperature was evaluated by fixing the acid concentration of the solutions at 15 mM. As shown in Fig. 3(a), the decomposition rate of PCC increased with increasing solvent temperature up to 230 °C. At 230 °C, the maximum liquid yield of 70% was obtained with a 20 mins reaction. However, further increasing solvent temperature to 240 °C did not significantly affect either the decomposition rate or the final liquid yield. Regardless of the solvent temperatures, the solid yields were stable at prolonged reaction times.

In Fig. 3(b), LGO and furfural yields both increased by the increasing solvent temperatures. The maximum LGO yield of 19.2% and furfural yield of 8.3% were achieved with the solvent temperature of 230 °C after a 20 mins reaction. Although the time to reach its optimal yield reduced with the solvent temperature of 240 °C, the yields of LGO and furfural did not exceed the maximum yields obtained from the 230 °C case. As shown in Figure S2, DGP and LGA yields also increased along with temperatures, although they were still minor products compared to LGO and furfural.

3.1.3. *Effect of mass loading*

The effect of PCC loading was evaluated by comparing the mass loadings of 0.6%, 1.2%, and 1.8% using a 230 °C THF solution with 15 mM acid. As shown in Fig. 4(a), varying PCC loading had minimal effects on the final liquid yield. However, the initial decomposition rate of PCC was lower with the increased mass loading. With 1.8% mass loading, it took 30 mins to reach 69.7% of liquid yield, while a similar liquid yield

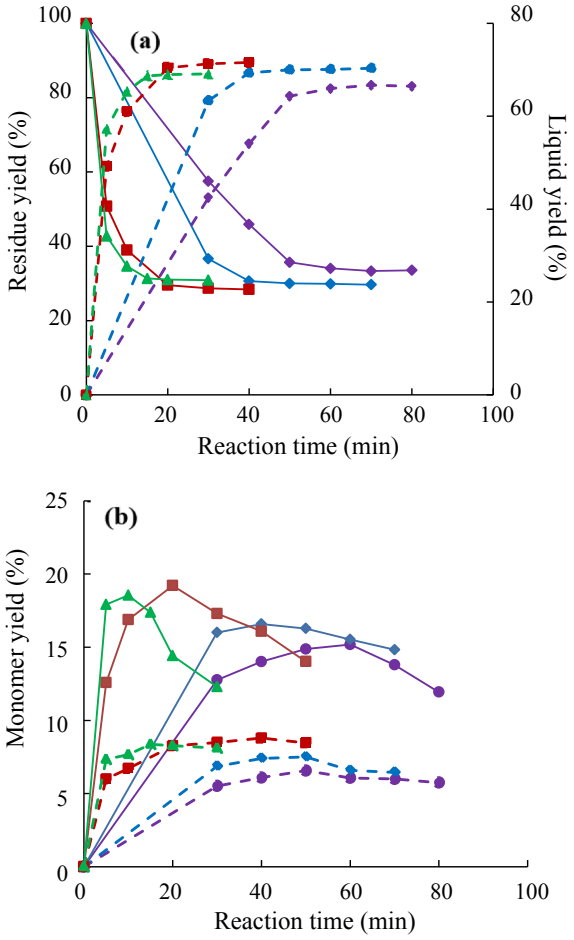

Fig. 3. Effect of solvent temperature during THF pretreatment of PCC with 15 mM acid. Purple lines with ◆: 210 °C; blue lines with ●: 220 °C; red lines with ■: 230 °C; green lines with ▲: 240 °C. (a) liquid (dotted lines) and solid yields (solid lines); (b) LGO (solid lines) and furfural yields (dotted lines). (For interpretation of the references to colour in this figure legend, the reader is referred to the web version of this article.)

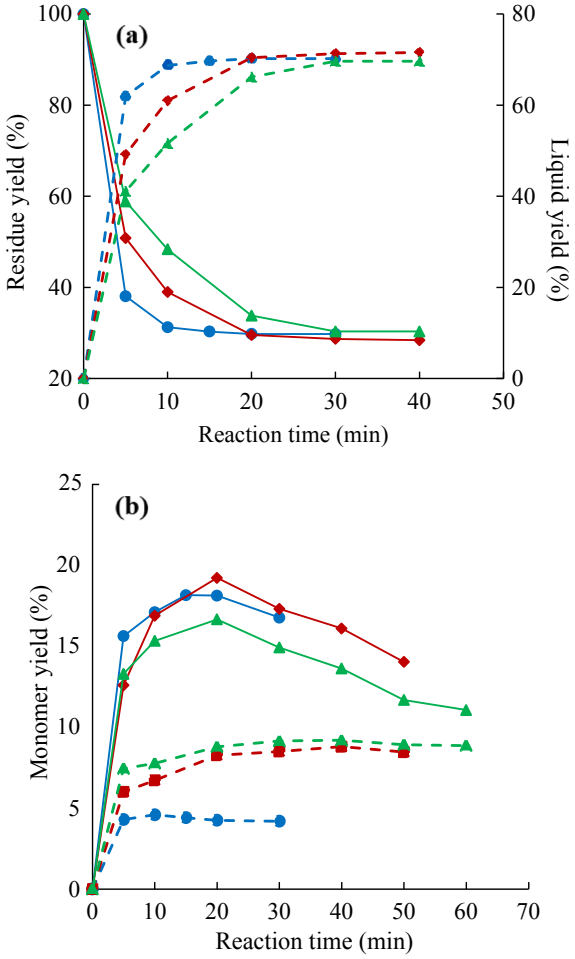

Fig. 4. Effect of PCC mass loading during THF pretreatment at 230 °C with 15 mM acid. Blue lines with ●: 0.6%; red line with ■: 1.2%; green lines with ▲: 1.8%. (a). liquid (dotted lines) and solid yields (solid lines); (b). LGO (solid lines) and furfural yields (dotted lines). (For interpretation of the references to colour in this figure legend, the reader is referred to the web version of this article.)

was achieved within a 10 mins reaction when PCC loading was 0.6%.

As shown in Fig. 4(b), increasing PCC loading reduced the optimal LGO yield from 19.2% with the 1.2% mass loading to 16.6% with the 1.8% mass loading. However, furfural yield was not affected by the changing PCC loading from 1.2% to 1.8%. On the other hand, employing the lowest PCC loading of 0.6% did not further increase LGO yield, although furfural yield was reduced noticeably. In Figure S3, a maximum DGP yield of 3.6% was obtained with 1.2% PCC loading. LGA yields remained very low at all PCC loadings. Overall, 1.2% PCC loading was the optimal mass loading to produce maximum monomer yields.

Noteworthy, no hydrocarbon products or nitrogen-containing compounds were detected in the liquids produced in all the above cases after the PCC was converted in the THF solutions. Thus, LDPE and PA in PCC remained as solids after the THF pretreatments. Since the synthetic polymers have much higher thermal stability than cellulose (Xue et al., 2017; Zulfiqar et al., 2010), the paper fraction was selectively decomposed during the THF treatment.

3.2. Evaluation of THF-pretreated solids

3.2.1. TGA analysis results

As shown above, pretreating PCC in THF solvents was able to selectively convert the paper fraction to produce up to 70% liquid products containing biobased chemicals. The THF-pretreated solids (TPS) with different THF temperatures were recovered at their respective optimal reaction times for reaching the maximum LGO yields, and their TGA results were shown in Fig. 5. The TGA results of the original PCC and the paper-removed carton (PRC) from the hydropulping of PCC were also included for comparison. As shown in Fig. 5(a), PCC volatilizes at two stages and leaves about 11% solid at 500 °C. Since the synthetic polymers in the PCC can completely volatilize, the solid residue was mainly derived from its paper fraction. As shown in Fig. 5(b), there were two distinctive DTG peaks (i.e., mass loss rate) in PCC. The first peak at a lower temperature region (<400 °C) corresponds to the decomposition of the paper fraction, and the second peak occurring at a higher temperature region (greater than400 °C) represents PE decomposition. The mass loss of PA usually occurs at slightly lower temperatures than PE (Sustaita-Rodríguez et al., 2019), but it is likely blended in the PE peak due to its low content in the PCC. Since the paper fraction was removed and thus PRC is a composite of PE and PA, its DTG includes a single mass loss peak at the high temperature region. All TPSs showed very similar TGA profiles. As it can be seen, there was also a single DTG peak for the TPSs, although the peaks were broader than that with PRC. The low-temperature mass loss related to the paper decomposition was mostly gone, whereas the high temperature peak representing PE and PA remained, confirming the selective decomposition of the paper fraction by the THF pretreatment. The temperatures corresponding to their respective maximum mass loss rates were nearly identical for all TPSs,

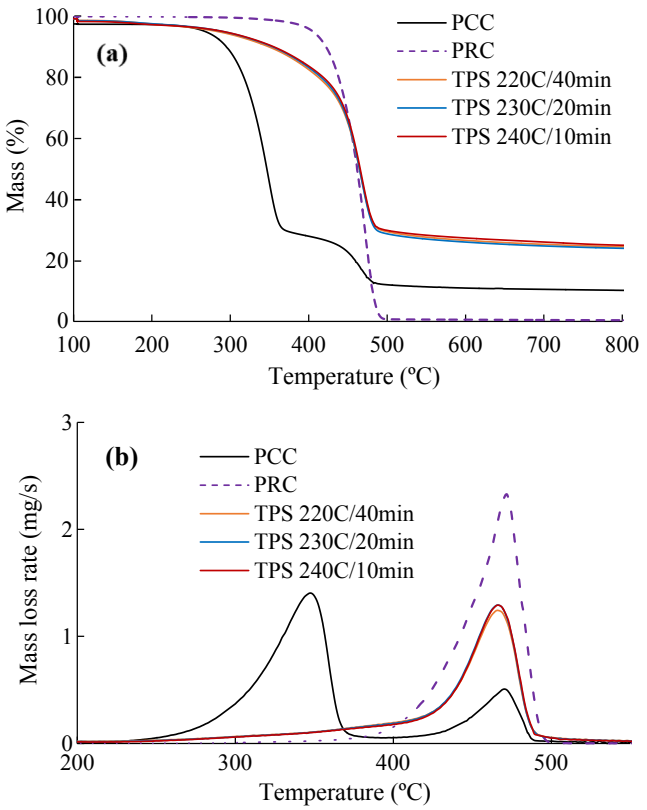

Fig. 5. (a) TGA and (b) DTG results of PCC, PRC, and TPSs.

PCC, and PRC, about 471–472 °C. In the TGA results of the TPSs, there were about 30% of solid residue at temperatures at 500 °C or above. Since PE and PA can completely devolatilize, the solids remaining during the TGA analysis of TPSs are originated from paper, produced during the THF pretreatment. While cellulose in the paper largely liquefies during the solvent pretreatment, carbonized solid residue was also produced in a smaller fraction due to the occurrence of condensation reactions. The cellulose-derived carbonized char has high thermal stability due to its polyaromatic condensed structure. From the above results, it is determined that TPS consists of PE, PA, and the paper-derived char.

3.2.2. FTIR analysis results

From the above, the TPS produced using 230 °C THF, 15 mM acid, 20 min reaction time was further subjected to the solvent dissolution method described in section 2.3 above to obtain a xylene-soluble TPS (i.e., XS-TPS) and a xylene-insoluble TPS (i.e., XIS-TPS). In Fig. 6, the FTIR spectrum of XS-TPS and PRC were compared. In PRC, the bands at 2846, 2914, and 1462 cm^{-1} standing for methyl and methane groups are originated from PE. Additionally, the band at 1575 cm^{-1} represents C = O and N-H, and the band at 1539 cm^{-1} is for C-N and N-H bending. The presence of the PA-derived bands confirms that PRC includes both PE and PA. In comparison, the PA-related bonds were completely absent, whereas the PE-related bonds remained in XS-TPS. The result shows that PE and PA in the TPS were separated after the solvent-dissolution treatment and by which PE was recovered as XS-TPS, whereas PA and the paper-derived char remained as XIS-TPS. In XS-TPS, the small peak at 1710 cm^{-1} representing carbonyl C = O is possibly due to the slight oxidation of PE during the THF pretreatment.

3.2.3. Pyrolysis-GC/MS and elemental analysis results

PRC, TPS, and XS-TPS were pyrolyzed to compare the GC chromatograms. As shown in Figure S4, pyrolysis of PRC produced a series of alkanes and olefins as they are typical products from PE depolymerization. Caprolactam was also found along with the hydrocarbon products. Since caprolactam is a PA-derived monomer, it is originated from PA in PRC. In comparison, the pyrolysis products of XS-TPS shown in Fig. 7(a) were PE-derived hydrocarbons. Caprolactam was not observed, which further confirms that PA was removed and XS-TPS is consisted of PE. Compared to PRC which is mixed polymers, XS-TPS can make a higher-quality feedstock for energy applications. Since it is basically PE, XS-TPS can be pyrolyzed to produce liquid hydrocarbon fuel molecules or combusted as a cleaner and higher energy density fuel.

The GC/MS spectrum of XIS-TPS pyrolysis shown in Fig. 7(b) has the dominant peak of caprolactam originated from PA decomposition. Other product peaks were very low, suggesting the volatile product was nearly exclusively caprolactam. Although the paper-derived char from the THF pretreatment also remains in XIS-TPS, they are thermally stable with low volatility, as described above. Recovering caprolactam from waste materials has been of interest as it is the precursor monomer in nylon-6

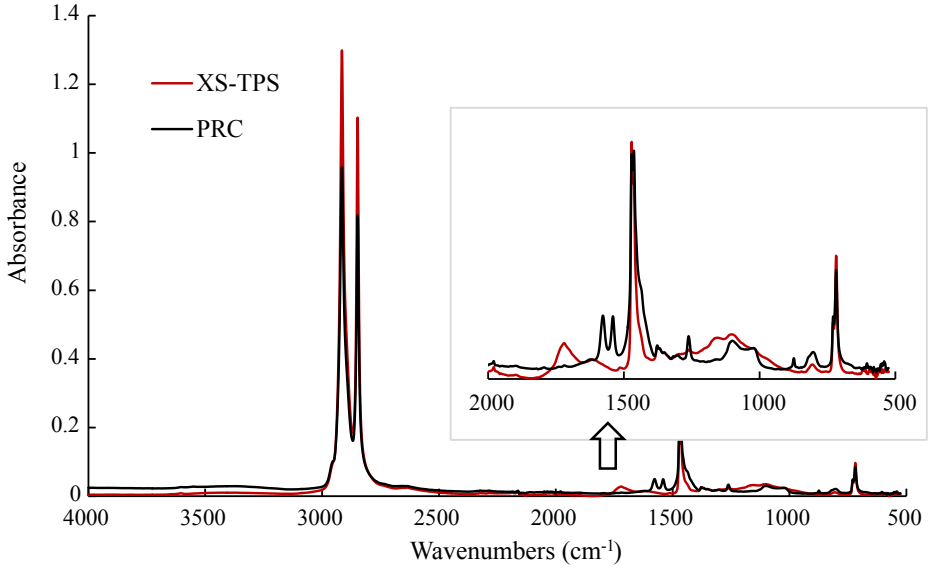

Fig. 6. FTIR spectrum of PRC and XS-TPS (obtained from TPS produced at 230 °C THF, 15 mM acid, 20 min reaction time. Same for the rest of the figures). The insert is zoomed-in.

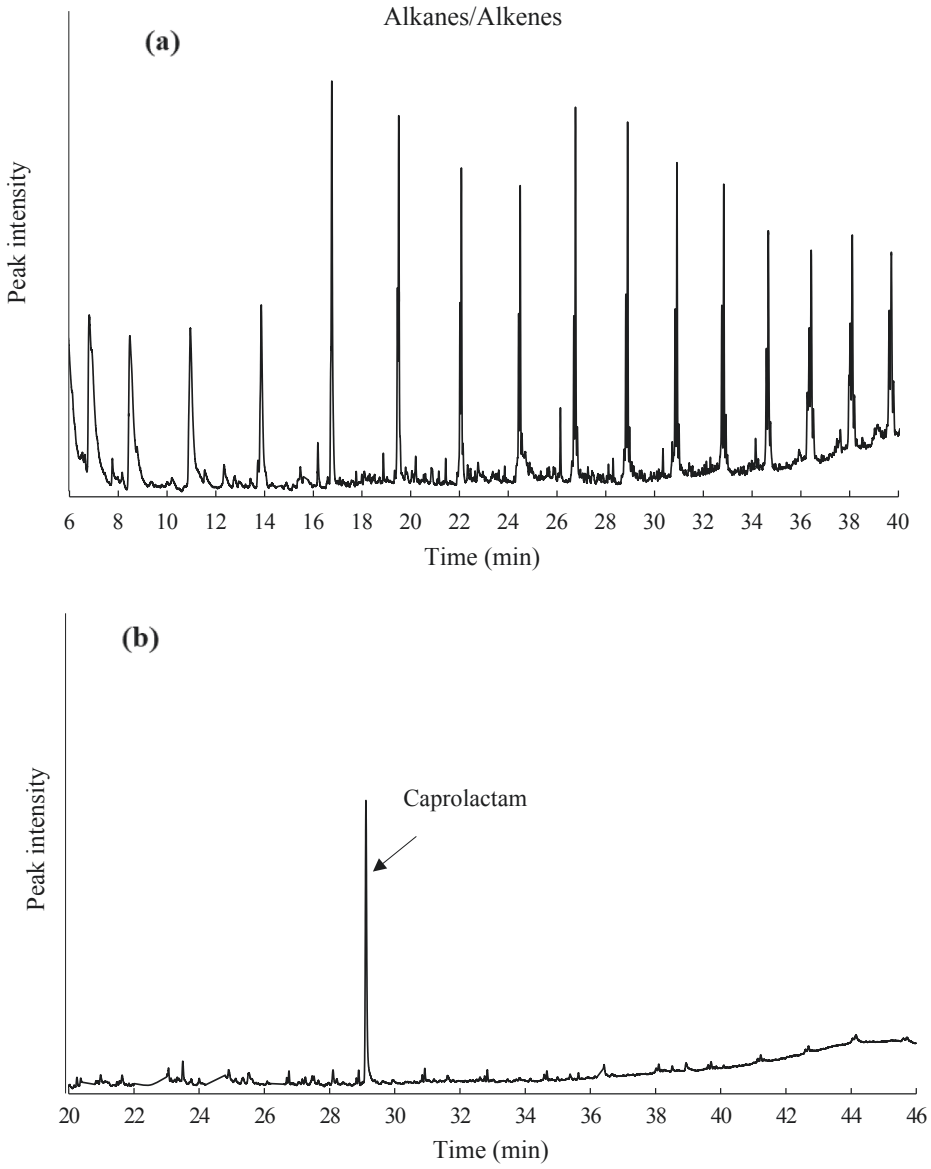

Fig. 7. Pyrolysis GC/MS chromatograms of (a) XS-TPS, and (b) XIS-TPS.

synthesis (Chen et al., 2013; Czernik et al., 1998; He et al., 2004; Xu et al., 2013). Based on the approach presented in this study, caprolactam with relatively high purity could be recovered by pyrolyzing XIS-TPS and condensing the vapor.

The elemental analysis results of XIS-TPS are given in Table S2. Compared to the results presented in Table S1 for PCC, XIS-TPS had an increased carbon content and a lower oxygen content due to the paper-derived char in this product. The nitrogen in XIS-TPS was originated from PA. The HHV of XIS-TPS was 22.17 MJ/kg, higher than 17.53 MJ/kg for PCC. Thus, the paper-derived char in XIS-TPS could also be considered as a solid fuel or other applications such as biochar or absorbent as these applications were already explored in previous studies (Ayiania et al., 2019; Sotoudehnia et al., 2020).

3.2.4. *Melt rheology of recycled plastics*

Other than being used as an energy source, the synthetic polymers recycled from PCC could be reapplied as polymers or composite materials (Kaiser et al., 2017; Robertson, 2021). As melt processibility is important in processing recycled polymers, PRC and XS-TPS were both subjected to isochronal temperature sweep scans to evaluate their melt rheology. The results are given in Fig. 8. In rheologic measurement, storage modulus (G') represents the elastic property of a material whereas loss modulus (G″) represents the viscous property. In Fig. 8(a), G″ became higher than G' at 132 °C for XS-TPS, indicating it turns into viscous material due to PE melting. The G' was higher than the G″ at a higher temperature region until they crossed at 232 °C. The transition of a viscous material to an elastic material at this temperature is due to crosslinking of the recycled PE. The complex viscosity (η*) of XS-TPS remains low for the tested temperature range. It decreased with increasing temperature until the polymer property degrades at 230 °C and above. The polymer chain session followed by radical coupling of the chain fragment ends develop a crosslinked structure, therefore severely limiting the flowability of the polymer due to its restricted structure. The above results suggest that the recycled PE obtained from this study (i.e., XS-TPS) has excellent melt processability at low temperatures. The rheology results of PRC are given in Fig. 8(b). The G' was higher than the G″ in a wide temperature range, although their values approached each other at temperatures of 219 °C and above. The corresponding η* of PRC was also much higher than that of XP-TPS until the temperature reaches 222 °C. Thus, PRC was an elastic material that was not melt-processible at the given temperature range. This is because the melting temperature of PA in PRC is 255–268 °C, higher than the

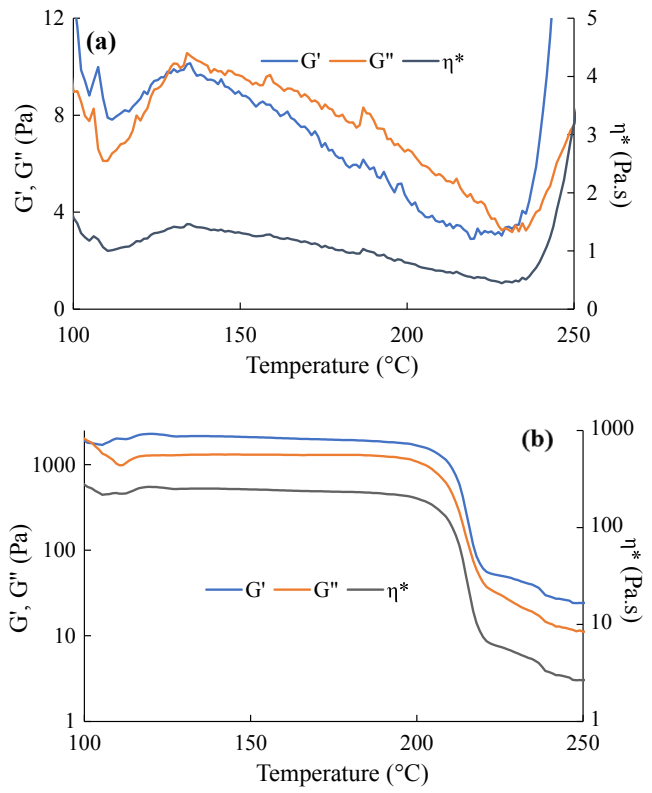

Fig. 8. Isochronal temperature sweep scans of (a) XS-TPS and (b) PRC.

maximum temperature used during the rheology test.

3.3. Advancement of the state of the art

As described in the introduction, prior-art approaches downcycled PCC to lower-value products (e.g., pulps, solid char, low-quality fuels) and/or only utilized selective compositions of PCC. In the present study, we explored a new approach to upcycle PCC, thereby maximizing the values of the final products. The PCC used in the present study belong to chilled package category, according to the Tetra Pak manufacturer. This specific PCC used for storing popular dairy products did not contain aluminum but PA in addition to paper and LDPE. Due to the polymer properties of PA and LDPE, it is more challenging to recycle this kind of PCC. The advancement in our recycling approach compared to prior arts is listed below:

1) High-valued biobased chemicals (e.g., $10,000/ton for LGO) were produced from PCC using a single step process without pretreatments. It should be noted that none of the previous recycling approaches produced chemicals using PCC. While the chemicals (other than caprolactam) are originated from the cellulose fraction, the presented single step approach is much more effective than converting hydropulped paper. For hydropulping, PCC needs to be soaked in water for hours. The pulp fibers are then filtered and dried before they could be used as a cellulosic feedstock for chemical production. In comparison, the single-step conversion does not need to deal with energy-intensive water evaporation and wastewater treatment. Furthermore, high monomer yields were obtained from PCC using short reaction times. Thus, the presented work provides an energy efficient, conversion effective, rapid and simple approach for obtaining high-value chemicals from PCC. Since this process selectively decomposes paper without impacting the plastic compositions in PCC, other fractions of PCC could also be recycled.
2) By using the non-polar solvent-based dissolution, PE and PA could be recovered separately from the solid residue of the pretreated PCC after the biobased monomers were produced. The recovered PE could be used as a new plastic material or the feedstock of high-quality hydrocarbon fuels; The insoluble fraction containing PA and paper-derived char (XIS-TPS) could be directly pyrolyzed to recover caprolactam in high selectivity. The high selectivity of caprolactam was possible because paper-derived char fraction was thermally stable during pyrolysis. In comparison, pyrolyzing either PCC or the paper-removed PCC would produce complex oils containing low-selectivity caprolactam mixed with paper and PE-derived organic molecules. Recovering caprolactam from such mixture oils is significantly more challenging than the presented approach.
3) The presented recycling approach could also be applied to aluminum-containing PCC. When the same process is employed, aluminum would end up in XIS-TPS along with PA and paper-derived char. After pyrolyzing XIS-PS to recover caprolactam, the aluminum and paper-derived char could be separated by their density difference.

4. Conclusions

Post-consumer carton packagings consisting of paper, PE, and PA were upcycled using a two-step approach. The pre-conversion of PCC in THF using dilute acid as catalyst produced up to 70% liquid consisting of LGO, furfural, DGP, and LGA. The acid concentration, solvent temperature and PCC mass loading could be optimized to increase the monomer yields, although the maximum liquid yield was not significantly affected by the pretreatment conditions. In this study, the maximum LGO yield of 19.2% and furfural yield of 8.3% were obtained directly from the carton by converting it using the solvent temperature of 230 °C and acid concentration of 15 mM. The TPS was a mixture of unreacted PE, PA, and paper-derived char residue. This solid was further separated into XS-TPS fraction and XIS-TPS by dissolving it in xylene. The FTIR analysis and the compositions of its pyrolysis products suggested that XS-TPS is a recycled PE. On the other hand, pyrolysis of XIS-TPS consisting of PA and paper-derived char almost exclusively produced caprolactam as the major vapor product with the remaining char could be used as solid fuel. Melt rheology results showed that the recycled PE could easily be melt-processed at temperatures above 130 °C. In comparison, the plastic fraction remaining after the hydropulping was not melt-processable at temperatures below 250 °C due to the high melting temperature of PA in the PE and PA composite. In future work, the economics of the recycling process should also be evaluated.

Declaration of Competing Interest

The authors declare that they have no known competing financial interests or personal relationships that could have appeared to influence the work reported in this paper.

Acknowledgement

The research is supported by National Science Foundation (grants no. 1803823 and 1826978).

Appendix A. Supplementary material

Supplementary data to this article can be found online at https://doi.org/10.1016/j.wasman.2021.06.031.

References

Lusi, A., Hu, H., Bai, X., 2020. Producing high yield of levoglucosan by pyrolyzing nonthermal plasma-pretreated cellulose. Green Chem. 22, 2036–2048. https://doi.org/10.1039/d0gc00255k.

Achilias, D.S., Roupakias, C., Megalokonomos, P., Lappas, A.A., Antonakou, E.V., 2007. Chemical recycling of plastic wastes made from polyethylene (LDPE and HDPE) and polypropylene (PP). J. Hazard. Mater. 149, 536–542. https://doi.org/10.1016/j.jhazmat.2007.06.076.

Achilias, D.S., Giannoulis, A., Papageorgiou, G.Z., 2009. Recycling of polymers from plastic packaging materials using the dissolution–reprecipitation technique. Polym. Bull. 63, 449–465. https://doi.org/10.1007/s00289-009-0104-5.

Ayiania, M., Terrell, E., Dunsmoor, A., Carbajal-Gamarra, F.M., Garcia-Perez, M., 2019. Characterization of solid and vapor products from thermochemical conversion of municipal solid waste woody fractions. Waste Manage. 84, 277–285. https://doi.org/10.1016/j.wasman.2018.11.042.

Bai, X., Brown, R.C., Fu, J., Shanks, B., Kieffer, M., 2014. The influence of alkali and alkaline earth metals and the role of acid pretreatments in production of sugars from switchgrass based on solvent liquefaction. Energy Fuels 28 (2), 1111–1120. https://doi.org/10.1021/ef4022015.

Lokahita, Baskoro, Aziz, Muhammad, Yoshikawa, K., Takahashi, F., 2017. Energy and resource recovery from Tetra Pak waste using hydrothermal treatment. Appl. Energy 207, 107–113. https://doi.org/10.1016/j.apenergy.2017.05.141.

Braden, J., Bai, X., 2018. Production of biofuel precursor chemicals from the mixture of cellulose and polyvinylchloride in polar aprotic solvent. Waste Manage. 78, 894–902. https://doi.org/10.1016/j.wasman.2018.07.011.

Cai, C.M., Nagane, N., Kumar, R., Wyman, C.E., 2014. Coupling metal halides with a co-solvent to produce furfural and 5-HMF at high yields directly from lignocellulosic biomass as an integrated biofuels strategy. Green Chem. 16, 3819–3829. https://doi.org/10.1039/c4gc00747f.

Cai, C.M., Zhang, T., Kumar, R., Wyman, C.E., 2013. Integrated furfural production as a renewable fuel and chemical platform from lignocellulosic biomass. J. Chem. Technol. Biotechnol. 89, 2–10. https://doi.org/10.1002/jctb.4168.

Cao, F., Schwartz, T.J., McClelland, D.J., Krishna, S.H., Dumesic, J.A., Huber, G.W., 2015. Dehydration of cellulose to levoglucosenone using polar aprotic solvents. Energy Environ. Sci. 8, 1808–1815. https://doi.org/10.1039/c5ee00353a.

Carton Facts [WWW Document], n.d. [WWW Document]. Carton Council. URL https://www.recyclecartons.ca/cartons-101/ (accessed 5.29.21).

Chen, D.Xuan, OuYang, X.Kun, Wang, Y.Guang, Yang, L.Ye, He, C.Hong, 2013. Liquid–liquid extraction of caprolactam from water using room temperature ionic liquids. Sep. Purif. Technol. 104, 263–267. https://doi.org/10.1016/j.seppur.2012.11.035.

Corne, V., Botta, M.C., Giordano, E.D., Giri, G.F., Llompart, D.F., Biava, H.D., Sarotti, A.M., Mangione, M.I., Mata, E.G., Suárez, A.G., Spanevello, R.A., 2013. Cellulose recycling as a source of raw chirality. Pure Appl. Chem. 85, 1683–1692. https://doi.org/10.1351/pac-con-12-11-10.

Czernik, S., Elam, C.C., Evans, R.J., Meglen, R.R., Moens, L., Tatsumoto, K., 1998. Catalytic pyrolysis of nylon-6 to recover caprolactam. J. Anal. Appl. Pyrol. 46, 51–64. https://doi.org/10.1016/s0165-2370(98)00068-0.

Delvere, I., Iltina, M., Shanbayev, M., Abildayeva, A., Kuzhamberdieva, S., Blumberga, D., 2019. Evaluation of Polymer Matrix Composite Waste Recycling Methods. Environ. Climate Technol. 23, 168–187. https://doi.org/10.2478/rtuect-2019-0012.

European Commission, LIFE Program - Project CLEAN: Converting Laminates Into Energy and Aluminium for the Benefit of Nature, LIFE06 ENV/E/000010.

Georgiopoulou, I., Pappa, G.D., Vouyiouka, S.N., Magoulas, K., 2021. Recycling of post-consumer multilayer Tetra Pak® packaging with the Selective Dissolution-Precipitation process. Resour. Conserv. Recycl. 165, 105268 https://doi.org/10.1016/j.resconrec.2020.105268.

Ghosh, A., Bai, X., Brown, R.C., 2018. Solubilized Carbohydrate Production by Acid-Catalyzed Depolymerization of Cellulose in Polar Aprotic Solvents. ChemistrySelect 3, 4777–4785. https://doi.org/10.1002/slct.201800764.

Ghosh, A., Brown, R.C., Bai, X., 2016. Production of solubilized carbohydrate from cellulose using non-catalytic, supercritical depolymerization in polar aprotic solvents. Green Chem. 18, 1023–1031. https://doi.org/10.1039/c5gc02071a.

He, C.-H., Gao, Y.-H., Yang, S.-H., Edwards, D.W., 2004. Optimization of the process for recovering caprolactam from wastewater in a pulsed-sieve-plate column using green design methodologies. J. Loss Prev. Process Ind. 17, 195–204. https://doi.org/10.1016/j.jlp.2003.12.001.

He, J., Liu, M., Huang, K., Walker, T.W., Maravelias, C.T., Dumesic, J.A., Huber, G.W., 2017. Production of levoglucosenone and 5-hydroxymethylfurfural from cellulose in polar aprotic solvent–water mixtures. Green Chem. 19, 3642–3653. https://doi.org/10.1039/c7gc01688c.

Henshaw, J.M., Han, W., Owens, A.D., 1996. An Overview of Recycling Issues for Composite Materials. J. Thermoplast. Compos. Mater. 9, 4–20. https://doi.org/10.1177/089270579600900102.

Hu, B., Lu, Q., Wu, Y.Ting, Cui, W.Luan, Xie, M.Shu, Liu, J., Yang, Y.Ping, 2020. Insight into the formation mechanism of levoglucosenone in phosphoric acid-catalyzed fast pyrolysis of cellulose. J. Chem. 43, 78–89. https://doi.org/10.1016/j.jechem.2019.08.001.

Jambeck, J.R., Geyer, R., Wilcox, C., Siegler, T.R., Perryman, M., Andrady, A., Narayan, R., Law, K.L., 2015. Plastic waste inputs from land into the ocean. Science 347, 768–771. https://doi.org/10.1126/science.1260352.

Kaiser, K., Schmid, M., Schlummer, M., 2017. Recycling of Polymer-Based Multilayer Packaging: A Review. Recycling 3, 1. https://doi.org/10.3390/recycling3010001.

Kamal, M.R., Jinnah, I.A., Utracki, L.A., 1984. Permeability of oxygen and water vapor through polyethylene/polyamide films. Polym. Eng. Sci. 24, 1337–1347. https://doi.org/10.1002/pen.760241711.

Korkmaz, A., Yanik, J., Brebu, M., Vasile, C., 2009. Pyrolysis of the tetra pak. Waste Manage. 29, 2836–2841. https://doi.org/10.1016/j.wasman.2009.07.008.

Krauklis, A.E., Karl, C.W., Gagani, A.I., Jørgensen, J.K., 2021. Composite Material Recycling Technology—State-of-the-Art and Sustainable Development for the 2020s. J. Composites Sci. 5, 28. https://doi.org/10.3390/jcs5010028.

Kudo, S., Goto, N., Sperry, J., Norinaga, K., Hayashi, J.-ichiro, 2016. Production of Levoglucosenone and Dihydrolevoglucosenone by Catalytic Reforming of Volatiles from Cellulose Pyrolysis Using Supported Ionic Liquid Phase. ACS Sustainable Chem. Eng. 5, 1132–1140. https://doi.org/10.1021/acssuschemeng.6b02463.

Kudo, S., Zhou, Z., Norinaga, K., Hayashi, J.-ichiro, 2011. Efficient levoglucosenone production by catalytic pyrolysis of cellulose mixed with ionic liquid. Green Chem. 13, 3306. https://doi.org/10.1039/c1gc15975e.

Lopes, C.M., Felisberti, M.I., 2006. Composite of low-density polyethylene and aluminum obtained from the recycling of postconsumer aseptic packaging. J. Appl. Polym. Sci. 101, 3183–3191. https://doi.org/10.1002/app.23406.

Lu, Q., Ye, X.Ning, Zhang, Z.Bo, Dong, C.Quing, Zhang, Y., 2014. Catalytic fast pyrolysis of cellulose and biomass to produce levoglucosenone using magnetic $SO_{42}-/TiO_2–Fe_3O_4$. Bioresour. Technol. 171, 10–15. https://doi.org/10.1016/j.biortech.2014.08.075.

Sarotti, M.A., Zanardi, M., Spanevello, A.R., 2012. Recent Applications of Levoglucosenone as Chiral Synthon. Curr. Org. Synth. 9, 439–459. https://doi.org/10.2174/157017912802651401.

Machado, G., Leon, S., Santos, F., Lourega, R., Dullius, J., Mollmann, M., Eichler, P., 2016. Literature Review on Furfural Production from Lignocellulosic Biomass. Nat. Resources 07, 115–129. https://doi.org/10.4236/nr.2016.73012.

Martínez-Barrera, G., De la Colina-Martínez, A.L., Martínez-López, M., del Coz-Díaz, J.J., Gencel, O., Ávila-Córdoba, L., Barrera-Díaz, C.E., Varela-Guerrero, V., Martínez-López, A., 2019. Recovery and Reuse of Waste Tetra Pak Packages by Using a Novel Treatment. Trends in Beverage Packaging 303–341. https://doi.org/10.1016/b978-0-12-816683-3.00011-6.

Mellmer, M.A., Sener, C., Gallo, J.M., Luterbacher, J.S., Alonso, D.M., Dumesic, J.A., 2014. Solvent Effects in Acid-Catalyzed Biomass Conversion Reactions. Angew. Chem. 126, 12066–12069. https://doi.org/10.1002/ange.201408359.

Müller, C., Gomez-Zurita Frau, M.A., Ballinari, D., Colombo, S., Bitto, A., Martegani, E., Airoldi, C., van Neuren, A.S., Stein, M., Weiser, J., Battistini, C., Peri, F., 2009. Design, Synthesis, and Biological Evaluation of Levoglucosenone-Derived Ras Activation Inhibitors. ChemMedChem 4, 524–528. https://doi.org/10.1002/cmdc.200800416.

Ostermeier, M., Schobert, R., 2014. Total Synthesis of (+)-Chloriolide. J. Organic Chem. 79, 4038–4042. https://doi.org/10.1021/jo500527g.

Pappa, G., Boukouvalas, C., Giannaris, C., Ntaras, N., Zografos, V., Magoulas, K., Lygeros, A., Tassios, D., 2001. The selective dissolution/precipitation technique for polymer recycling: a pilot unit application. Resour. Conserv. Recycl. 34, 33–44. https://doi.org/10.1016/s0921-3449(01)00092-1.

Platnieks, O., Barkane, A., Ijudina, N., Gaidukova, G., Thakur, V.K., Gaidukovs, S., 2020. Sustainable tetra pak recycled cellulose / Poly(Butylene succinate) based woody-like composites for a circular economy. J. Cleaner Prod. 270, 122321 https://doi.org/10.1016/j.jclepro.2020.122321.

Polprasert, C., 2007. Organic waste recycling. Amer Welding Society.

Popelka, A., Krupa, I., Novák, I., Al-Maadeed, M.A., Ouederni, M., 2016. Improvement of aluminum/polyethylene adhesion through corona discharge. J. Phys. D Appl. Phys. 50, 035204 https://doi.org/10.1088/1361-6463/50/3/035204.

Raclavská, H., Růžičková, J., Škrobánková, H., Koval, S., Kucbel, M., Raclavský, K., Švédová, B., Pavlík, P., Juchelková, D., 2018. Possibilities of the utilization of char from the pyrolysis of tetrapak. J. Environ. Manage. 219, 231–238. https://doi.org/10.1016/j.jenvman.2018.05.002.

Robertson, G., 2021. Recycling of Aseptic Beverage Cartons: A Review. Recycling 6, 20. https://doi.org/10.3390/recycling6010020.

Siddiqui, M.Z., Han, T.U., Park, Y.-K., Kim, Y.-M., Kim, S., 2020. Catalytic Pyrolysis of Tetra Pak over Acidic Catalysts. Catalysts 10, 602. https://doi.org/10.3390/catal10060602.

Sotoudehnia, F., Baba Rabiu, A., Alayat, A., McDonald, A.G., 2020. Characterization of bio-oil and biochar from pyrolysis of waste corrugated cardboard. J. Anal. Appl. Pyrol. 145, 104722 https://doi.org/10.1016/j.jaap.2019.104722.

Sustaita-Rodríguez, J.M., Medellín-Rodríguez, F.J., Olvera-Mendez, D.C., Gimenez, A.J., Luna-Barcenas, G., 2019. Thermal Stability and Early Degradation Mechanisms of High-Density Polyethylene, Polyamide 6 (Nylon 6), and Polyethylene Terephthalate. Polym. Eng. Sci. 59, 2016–2023. https://doi.org/10.1002/pen.25201.

Tetra Pak International, 2020d, Tetra Pak carton 100% Recyclable. Retrieved from https://www.tetrapak.com/in/sustainability/good-for-you-good-for-the-earth/tetra-pak-cartons-fully-recyclable.

Weingarten, R., Rodriguez-Beuerman, A., Cao, F., Luterbacher, J.S., Alonso, D.M., Dumesic, J.A., Huber, G.W., 2014. Selective Conversion of Cellulose to Hydroxymethylfurfural in Polar Aprotic Solvents. ChemCatChem 6, 2229–2234. https://doi.org/10.1002/cctc.201402299.

Xing, L., Gu, J., Zhang, W., Tu, D., Hu, C., 2018. Cellulose I and II nanocrystals produced by sulfuric acid hydrolysis of Tetra pak cellulose I. Carbohydr. Polym. 192, 184–192. https://doi.org/10.1016/j.carbpol.2018.03.042.

Xue, Y., Johnston, P., Bai, X., 2017. Effect of catalyst contact mode and gas atmosphere during catalytic pyrolysis of waste plastics. Energy Convers. Manage. 142, 441–451. https://doi.org/10.1016/j.enconman.2017.03.071.

Xu, Y., Tang, K., Bai, Z.S., Wang, H.L., 2013. Hydrodynamic and Mass-Transfer Characteristics of Annular Centrifugal Contactors on the Caprolactam Recovery from

Waste Liquor. Appl. Mech. Mater. 330, 792–798. https://doi.org/10.4028/www.scientific.net/amm.330.792.

Yang, Y., Boom, R., Irion, B., van Heerden, D.-J., Kuiper, P., de Wit, H., 2012. Recycling of composite materials. Chem. Eng. Process. Process Intensif. 51, 53–68. https://doi.org/10.1016/j.cep.2011.09.007.

Zawadiak, J., 2017. Tetra Pak Recycling – Current Trends and New Developments. Am. J. Chem. Eng. 5, 37. https://doi.org/10.11648/j.ajche.20170503.12.

Zhang, Z., Lu, Q., Ye, X., Wang, T., Wang, X., Dong, C., 2015. Selective Production of Levoglucosenone from Catalytic Fast Pyrolysis of Biomass Mechanically Mixed with Solid Phosphoric Acid Catalysts. Bioenergy Res. 8, 1263–1274. https://doi.org/10.1007/s12155-015-9581-6.

Zhao, Y., Lv, X., Ni, H., 2018. Solvent-based separation and recycling of waste plastics: A review. Chemosphere 209, 707–720. https://doi.org/10.1016/j.chemosphere.2018.06.095.

Zulfiqar, S., Ishaq, M., Ilyas Sarwar, M., 2010. Synthesis and characterization of soluble aromatic-aliphatic polyamide. Adv. Polym. Tech. 29, 300–308. https://doi.org/10.1002/adv.20197.